Polycyclic Aromatic Hydrocarbon Based Electrical Sensor: Dimethylamine Substituted Alkynylated Anthracene for H_2 Detection

Khadimul Islam,[a] Thomas T. Daniel,[b] Roy P. Paily,*[b,c,d] Akshai Kumar*[a,b,d]

[a]Department of Chemistry, Indian Institute of Technology Guwahati, Guwahati-781039, Assam, India.

[b]Center for Nanotechnology, Indian Institute of Technology Guwahati, Guwahati–781039, Assam, India.

[c]Department of Eectronics and Electrical Engineering, Indian Institute of Technology Guwahati, Guwahati - 781039, Assam, India.

[d]Jyoti and Bhupat Mehta School of Health Sciences and Technology, Indian Institute of Technology Guwahati, Guwahati-781039, Assam, India

KEYWORDS. Polycyclic Aromatic Hydrocarbons, π-Conjugated Organic Semiconductors, Electrical Sensors, Tetralkynylated Anthracene and Hydrogen Detection.

ABSTRACT: The demand for hydrogen is on a continuous rise in view of its application as a clean-burning and alternate carbon-free energy source. It is flammable at concentration above 4 % in air and is odorless. Fabrication of highly sensitive and selective hydrogen sensors based on small organic molecules which operate at room temperature is challenging. This work describes the fabrication of a hydrogen sensor containing π-conjugated organic semiconductor based on a *N*,*N*-dimethylamine substituted tetraalkynylatedanthracene that can detect H_2 at concentrations as low as 150 part per million (ppm) at room temperature. The *N*,*N*-dimethyl amine containing tetraalkynylatedanthracene (**AnPhNMe$_2$**) has been synthesized by tetra-fold Sonogashira reaction employing a catalyst system based on $Pd(CH_3CN)_2Cl_2$ + cataCXium® A. A precisely controlled fabrication is enabled by employing a *μ*-gridder printing system. The gas sensor shows excellent sensitivity, fast response and high recovery to H_2 at room temperature. Moreover, after the interaction with H_2, the surface electron of the $ANPhNMe_2$ gets enhanced and shows a decrease in the resistance of the fabricated device. Sensor exhibits a limit of detection of 49 ppb with the highest sensitivity of 19.95% for the detection of 900 ppm of H_2, with a response time of 10 to 20 seconds. This work aims to develop a proof-of-concept for enhancing room temperature hydrogen sensing by developing a low cost printed sensor.

Introduction

The availability of energy sources have a great impact on human life. Nowadays, the demand of energy has increased with increase in human population and industrial revolution. The main sources of energy are petroleum, coal, and natural gas.[1] The fossil fuels are non-renewable resources of energy and their combustion results in the emission of greenhouse gasses.[2] Over the years, air pollution has been a sensible concern due to the emission of hazardous and poisonous gases in the atmosphere which causes severe health diseases. Unlike combustion of fossil fuels, in fuel cell that converts H_2 to electrical energy[3] water is produced as the only side product without any CO_2 emission.[4]

Hence, currently, researchers are greatly focused on utilization of hydrogen gas as renewable energy source[4a, 5] for the future due to its abundance,[6] high gravimetric energy density,[5b, 6] and high efficiency of combustion.[4b] But, it is highly inflammable (lower flammable limit 4%),[1c] tasteless, odourless and colourless which possess a threat to human health.[7] Humans cannot sense the hydrogen gas and detection of its leakage is very difficult. The production, transport and storage of hydrogen is highly risky.[2, 8] For these reasons, the detection of H_2 with high selectivity as well as sensitivity is desirable.[7] The hydrogen sensors must be power-efficient, inexpensive and also functional in humidity at room temperature.[9]

In terms of detection method, gas sensors can be categorised as (i) variations on the electrical characteristics and (ii) variations in other characteristics.[10] In the first category, the sensor is fabricated based on semiconductors and works on electrical properties.[11] On the other hand, the gas can be measured by other parameters like thermal, optical, gas chromatography-mass spectroscopy, mechanical and acoustic.[12] Among the detection methods, electrical sensors based on semiconductors have received significant interest owing to their advantage in terms of easy assembly and intrinsic qualities of converting chemical or physical occurrences to the voluntarily observable electrical signal.[11a,13]

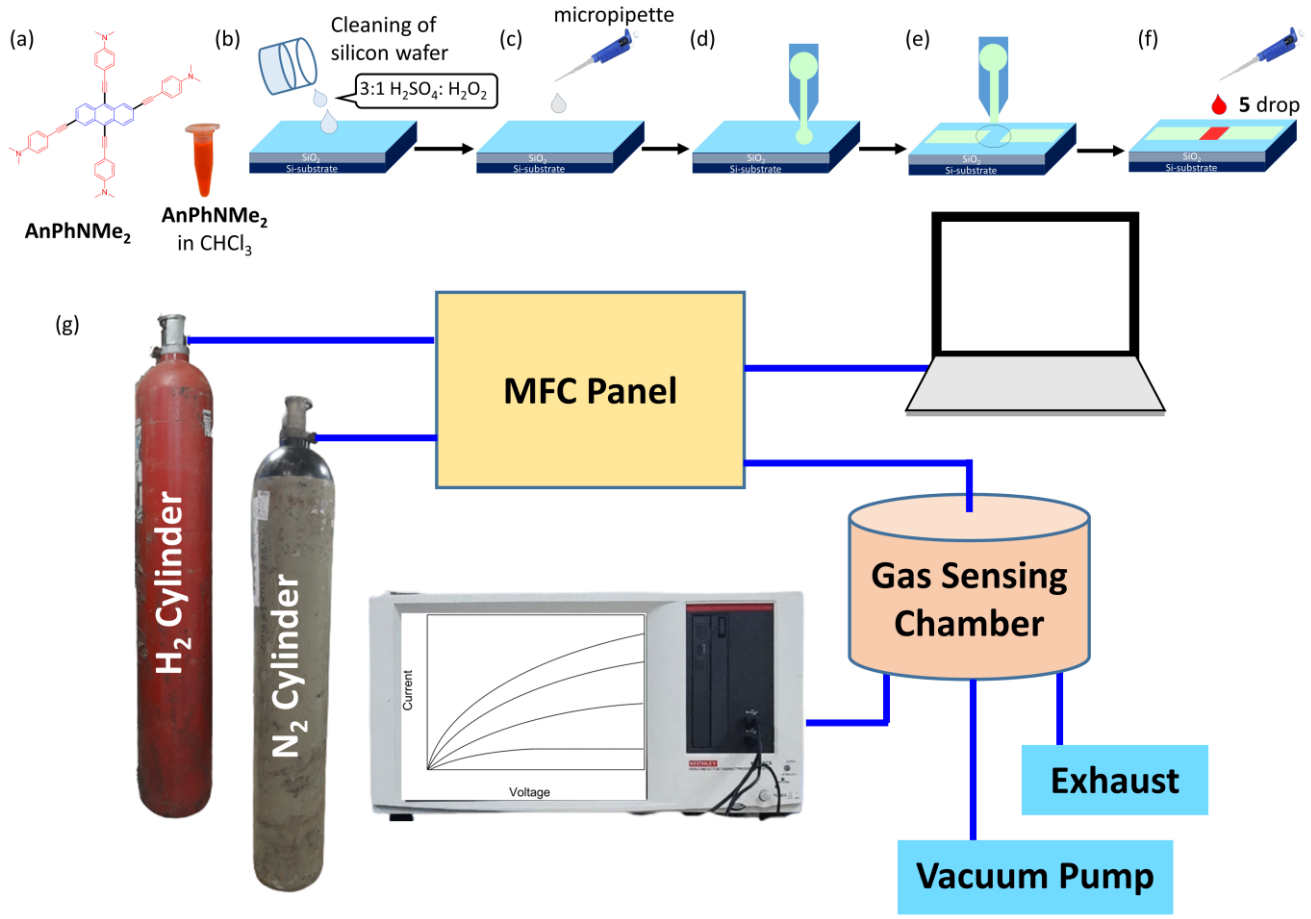

Figure 1. Fabrication steps of electrical devices (a) Structure of the **AnPhNMe$_2$**, (b) Cleaning of silicon wafer by piranha solution, (c) Drop casting the AgNP ink, (d) Placing *μ*-girder, (e) Patterning *μ*-girder, (f) Drop casting of **AnPhNMe$_2$**, (g) fabricated device connected to Keithly 2600 for sensing experiment.

Over the last decades, various types of semiconductors have been reported to detect hydrogen gas like metal oxide semiconducting materials,[1a, 1c, 9, 13c, 14] carbon-based materials[15] and conducting polymers.[16] The interaction of H_2 with the semiconductor improves the surface electron concentration and enhances the conductivity of the *n*-type semiconductor.[1a, 11a]

Scheme 1. The synthetic route of $AnPhNMe_2$ (**5**)[22a]

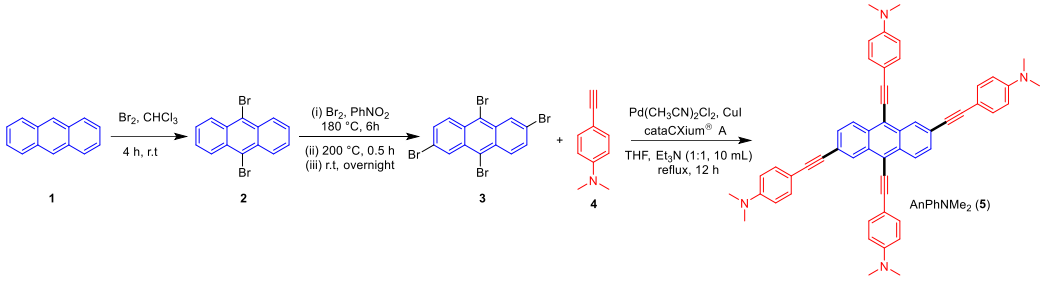

Undoubtedly, mostly metal oxide semiconductors like ZnO, TiO_2, SnO_2, WO_3, and V_2O_5 are used to detect hydrogen gas.[1a, 17] Metal oxide-based semiconductors have a wide band gap,[1a, 17b, 18] so it is incapable of exciting them spontaneously at room temperature.[19] One requires UV light or heating for excitation to overcome this barrier, which is a drawback in their broad application.[11a] Modification is required to detect hydrogen gas at room temperature by semiconductors-based sensors.[20] As a result, a semiconductor material with a low band gap is preferable for efficiently detecting hydrogen.

Organic semiconductors are widely used as active materials in electronic devices.[21] Extended *π*-conjugated polyaromatic hydrocarbons (PAHs) are promising candidates for fabricating an electronic device due to their solution processability, light weight, mechanical flexibility, low-cost of production, good film-forming ability, room temperature operation, and easily tailored functional group for sensing applications.[21a] Because of its environmental stability, electric conductivity, and intriguing redox properties associated with a nitrogen atom in the chain, polyaniline (PANI) and polypyrrole have been reported as a hydrogen sensor.[16] However, the development of hydrogen sensors based on metal-free organic semiconductors based on *π*-conjugated polyaromatic hydrocarbons (PAHs) remains a challenge. To the best of our knowledge, small *π*-conjugated organic compounds, have not been studied for their ability to detect hydrogen gas.

PAHs such as anthracene contain fused rigid three benzene ring and introduction of alkyne unit to anthracene moiety enhances its thermal stability, planarity and π-conjugation which are essential for intermolecular interaction and charge transport. Choi and co-workers have reported twelve PAHs based on unsymmetrical 2,6,9,10-tetraalkynylatedanthracene compounds and used them for the fabrication of OFETs devices.[21a] Recently our group reported a library of PAHs based on symmetrical 2,6,9,10-tetraalkynylatedanthracenes.[22] While 2,6,9,10-*tetrakis*(phenylethynyl)anthracene (CCDC 2070944)[22] and 2,6,9,10-*tetrakis*(*p*-tolylethynyl)anthracene (CCDC 2070945)[22] exhibit unsymmetrical T-shaped and symmetrical bifurcate C-H·····(C≡C) interactions involving both C_{sp2}-H donors and conjugated π_{alkyne} acceptors in solid state, such interactions are absent in 2,6,9,10-*tetrakis*(*N*,*N*-dimethylaniline-ethynyl)anthracene (CCDC 2070947) which contains $–PhNMe_2$ group which acts as a donor, acetylene unit that acts as a *π*-spacer and anthracene moiety behaves as an acceptor. Apart from exhibiting halochromism,[22] 2,6,9,10-*tetrakis*(*N*,*N*-dimethylaniline-ethynyl)anthracene also possesses a low band gap of 1.79 eV[22a] which offers immense promise as an organic semi-

conductor. Notably, the acetylene unit is capable of forming weak interactions with molecules like hydrogen, allowing one to make a high-quality sensor under room temperature conditions.

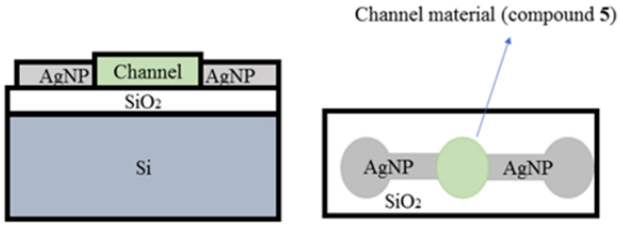

Figure 2. Schematic representation of the fabricated device

The microfabrication technique is also required for the development of low-cost organic semiconductor-based portable electronic devices.[23] This technique is widely used in a variety of industries to create small designs for property modification, patterning, subtractive and additive processes, and packaging. Traditional microfabrication technology is insufficient in terms of both money and time. As a result, developing a low-cost sensor will be difficult. Printing, on the other hand, is a relatively new microfabrication technique that has recently been investigated as an alternative to decades-old technology. The fabrication of device is printed using a low-cost additive manufacturing technology that operates at low temperature at ambient pressure by a maskless process and is environmentally friendly. The primary benefit of this technology is the reduced time required for device manufacturing, which enables rapid prototyping and device testing with minimal material waste. As a result, the cost of producing electronic devices is significantly reduced. It also ensures that low-volume and high-volume fabrication needs are met simultaneously and high-volume fabrication needs are met at the same cost.[24] As per our knowledge, this is the first time we report the a device which is fabricated by using μG printing technology for small organic semiconductor to gas sensing.

Experimental Section

Material and Instruments.

To carry out the printing experiments, a silver nanoparticle (AgNP) conductive ink (Product No. 736481), is purchased from Merck-India Pvt. We also purchased a Silicon wafer from university wafers. A calibrated cylinder containing 50000 ppm of H_2 in nitrogen was used for the sensing investigation. Anthracene, bromine, $Pd(CH_3CN)_2Cl_2$, cataCXium® A, CuI, 4-ethynyl-*N.,N*-dimethylaniline, Si, SiO_2, Ag were purchased from Sigma-Aldrich, Alfa-aesar. The chemicals was used without further purification. The solvent like, THF, Et_3N, $CHCl_3$, CH_2Cl_2 were purchased from Merck and used by drying or distillation. THF and Et_3N were dried via double distillation by using Na/benzophenone and KOH. NMR spectra were recorder by using 400 MHz for ^1H NMR and 101 or 151 MHz for $^{13}C\{^1H\}$ NMR Peak characterization: s = singlet, d = doublet, t = triplet. A Field Emission Scanning Electron Microscope (FESEM) [Make: JEOL, Model: JSM-7610F] is used to visualise the physical properties of the material. TEM image was captured by using Field Emission Transmission Electron Microscopy (FETEM) [Make JEOL, Model: JEM 2100F]. A high-resolution Rigaku TTRAX III 18 kW X-ray diffractometer was used to analyse the phase identification of the as-synthesized material.

Synthesis.

The target compound is synthesized by following the synthetic route as shown in Scheme 1. The compound **AnPhNMe$_2$** (**5**) was obtained via three step reaction according to our previous report.[22a,b] In the first step, 9,10-dibromoanthracene **2** was synthesized by the bromination of

anthracene using bromine in chloroform at room temperature. Subsequently, the precursor **3** was prepared by bromination of 9,10-dibromoanthracene **2**.[22] This was followed by the tetra-fold Sonogashira reaction of 2,6,9,10-tetrabromoanthracene **3** with 4-ethynyl-*N*,*N*-dimethylaniline **4** to yield the desired product **5**. The synthetic procedure and structural identification of the all the considered compounds **1-5** are described in ESI.

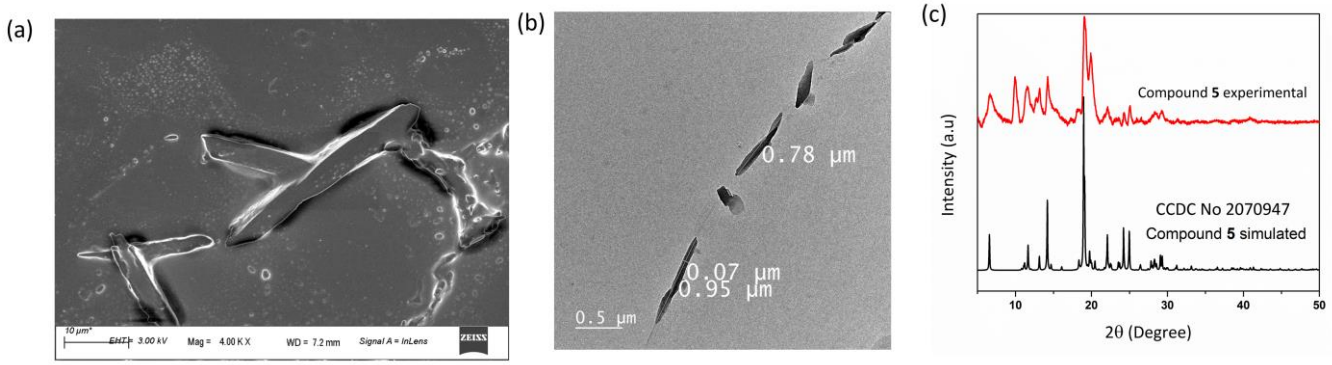

Figure 3. (a) Field emission scanning electron microscopy (FESEM) image of **5** (b) Field emission transmission electron microscope (FETEM) image of **5** (c) PXRD pattern of **5**

Fabrication process.

The sensor is developed on an undoped silicon/silicon oxide (Si/SiO_2) substrate that was exposed to UV light for 10 minutes prior to fabrication. A printing system (Make, Model: K-FAB TECH PRIVATE LIMITED, K-FT1PS) is used to control and optimise the fabrication of the metal contact pads. The system's printing head includes a stainless-steel micro girder patterning tool through which ink flows down to the substrate. The printing was carried out at room temperature and with a relative humidity of approximately 50 percent.

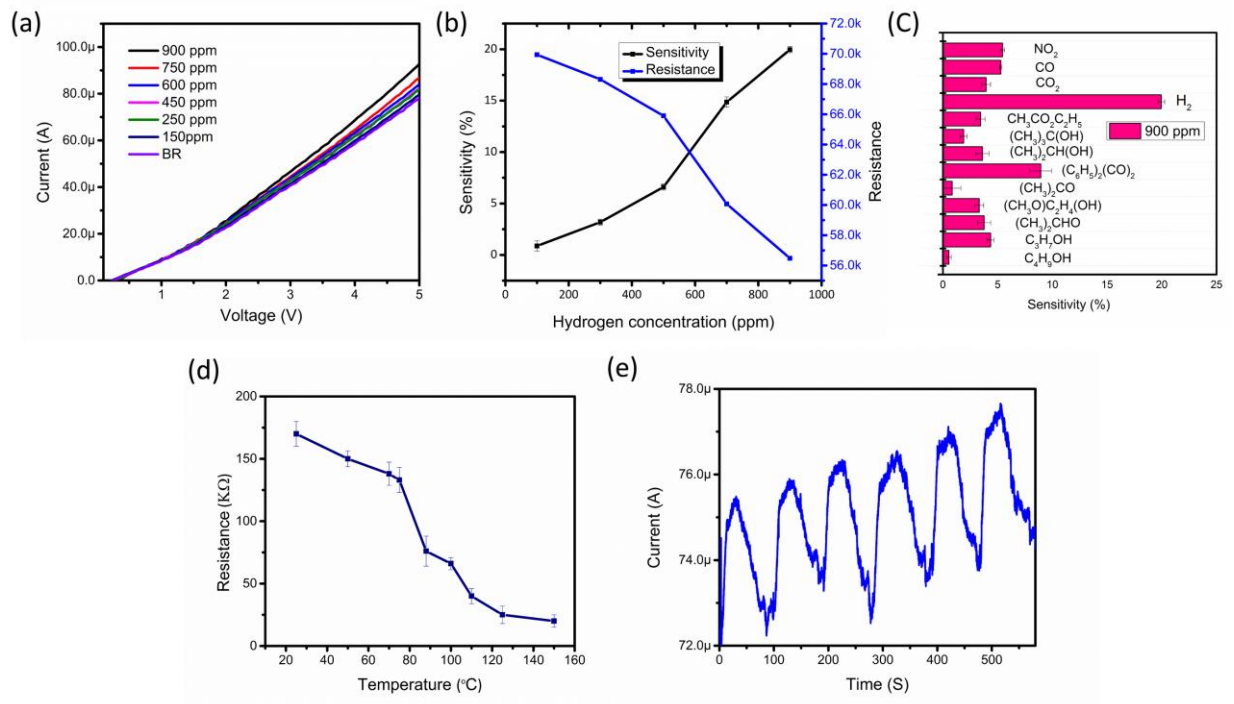

Figure 4. (a)The I-V characteristic of sensing devices, (b) Sensors' AER and sensitivity vs hydrogen concentration, (c) Sensor responses to various gases and VOCs (d) Temperature response of the sensor, (e) the sensor's transient response

Two distinct AgNP ink spots were drop-cast with a 1mm spacing on the SiO_2 substrate. The micro girder's tip is positioned to lightly tap AgNP ink on the upper surface of a spot. To close the gap, AgNP ink is dragged closer to the other spot. The second AgNP spot is then treated in the same manner, with the ink dragged closer to the previously printed electrode to reduce the channel gap to approximately 20 μm. For 20 minutes, the printed electrodes are gently heated at 160°C. The entire electrode fabrication process can be completed in 30 minutes with 2 μL of AgNP ink. The solution of **5** was prepared in DCM (1 mM). The channel material is then dropped cast over the printed AgNP electrodes, with a drop cast diameter of about 2 mm. After that, the device is annealed for five minutes at 120°C. The schematic of the fabricated device is shown in Figure 2

Figure 3a and b depicts the morphology of a sub-micron nanowire. Nanostructures, such as nanowires and nanocrystals morphology, provide new and sometimes unique opportunities for sensing biological and chemical species, and thus intuitively represent excellent primary transducers for signal production. We used Field Emission Transmission Electron Microscopy (FETEM) to examine the aspect ratio of sub-micron wires with a diameter of 0.07 micro m and a single crystal structure. Powder XRD analysis was done to analyse the phase identification of the **5**. Previously, we had reported the SCXRD of the **5** (CCDC No 2070947) and Figure 3 confirms that the material peaks are almost same as the simulated XRD pattern. This shows that the crystallinity and phase are intact in crystal as well as powder form (Figure 3c).

Results and discussion

Electrical characteristics.

The electrical properties of the fabricated devices were investigated using a Keithly 2600 source metre. A low-noise triaxial cable connects the device to the analyzer. To perform the sensing experiment, an in-house designed gas sensing system (Fabricator: Genrenew India) was connected to the above analyzer via low-noise triaxial cables. To achieve the desired gas concentration, the gas sensing chamber is outfitted with a Mass Flow Controller (MFC) panel composed of three MFCs with varying flow rates. The carrier gas flow is controlled by one MFC, while the other MFCs control the analyte gas flow. The sensing experiment is carried out in two conditions: (a) in nitrogen ambient and (b) in various hydrogen concentrations (H_2).

To avoid cross-contamination, the gas sensing chamber is purged with nitrogen before being evacuated three times. The baseline readings of the sensors were taken in a nitrogen environment with less than 1% humidity and close to atmospheric pressure. The I-V characteristic of sensing devices is examined by sweeping a voltage from 0 to 5 V. The device exhibits an ohmic response as shown in the figure 4a.

A series of experiments are carried out to evaluate the response of the devices by varying the concentration of hydrogen gas from 150 to 900 ppm. Figure 4a depicts the device's I-V characteristics for a sweeping voltage of 0 to 5 Volt with different hydrogen concentrations. The electrical properties confirm an increase in current with increasing hydrogen concentration. The interaction with H_2 gas reduces the device's resistance. Because H_2 is a reducing gas, interacting with it raises the concentration of surface electrons on electron rich $AnPhNMe_2$ semiconductors. The following equation was used to determine the response of the gas sensors.

$$S = (\lfloor R_g - R_o \rfloor / R_o) \text{ X } 100\% \qquad (1)$$

Where R_g is the average electrical resistance obtained by sweeping the voltage from 0 to 5V toward varying H_2 concentrations, and R_o is the average electrical resistance of the sensors in the nitrogen atmosphere. Figure 4b depicts the sensors' AER and sensitivity vs H_2 concentration plots. The AER response confirms that a significant shift in the fabricated device. According to the results, the sensor has a high sensitivity of 19.95 percent to 900 ppm and 0.86 percent to 50 ppm.

Figure 4c depicts the sensor's sensitivity to various gasses and volatile organic compounds (VOCs) at 900 ppm concentration. The desired VOC concentrations were achieved by combining it with deionized water and injecting it into the bubbler connected to the chamber. VOCs exhibit significantly lower responses than H_2 gas at the same concentration. When the sensor's limit of detection (LOD) is calculated using the equation 2, it shows a value of 49 ppm.

$$LOD = |\sigma|/slope \qquad (2)$$

Where slope denotes the average electrical resistance for the various analyte gas concentrations and σ is the standard deviation of the base reading.

For the sensor's response to temperature variation, a tightly sealed chamber was used. Initially, the chamber is kept at 20°C and then heated to 160°C to analyse the sensor characteristics related to resistance variation. Figure 4d depicts the variation of resistance with temperature. The resistance decreases significantly in the temperature range of 20 to 160 degrees Celsius. As a result, it is possible to conclude that the device's resistance decreases as the temperature rises. Temperature is an external factor that can affect the sensor.

Figure 4e depicts the sensor's transient response. The sensor was continuously flashed to seven pulses of H_2 gas at various concentrations of 100, 250, 400, 550, 700, and 900 ppm, accompanied by a mild evacuation of the gas in the sensing chamber at a constant voltage of 5 V. For different H_2 concentrations, the transient response provides an excellent response time ranging from 0 to 15 s with a good recovery time of 40 to 60 s. The gas in-conditioning process begins when the gas sensing chamber is pressurised to atmospheric pressure, and the gas out-conditioning process begins when the flow of the analyte gas is stopped and evacuated. A mild baseline shift was observed when the sensor shifted back and forth between mild vacuum and test gas environment.

Conclusions

This work employs a different fabrication approach to fabricate low-cost hydrogen gas sensors based on dimethylamine substituted alkynylated anthracene. The sensing response of all the devices is validated. The *μ* grider-based printing technology offers a simple method for creating low-cost, high-quality sensors. The specificity of the sensors was verified against some of VOCs. When the device is exposed to hydrogen gas, the surface electron of the π-conjugated organic semiconductor got enhanced and shows a good response and recovery time. Furthermore, the response and recovery of the sensor is excellent.

Conflicts of interest

The authors declare no conflict of interest

Acknowledgment

A.K. is grateful for the grants received from Science and Engineering Research Board (Grant No. DST-SERB CRG/2022/002354). A.K. acknowledges the Scheme for Transformational and

Advanced Research in Sciences, Ministry of Education, implemented by Indian Institute of Science (IISc), Bangalore (Grant No. STARS/APR2019/CS/629/FS). The funds received from Ministry of Electronics and Information Technology via the INUP-I2I program (5(1)/2021-NANO) and the SWASTHA COE (5(1)/2022-NANO) are gratefully acknowledged. Thanks are also due to the financial support from Indian Council of Medical Research, New Delhi (5/3/8/20/2019-ITR). The DST-FIST program, NECBH-IITG, Department of Chemistry at IITG and CIF-IITG are acknowledged for various instrumental facilities.

Abbreviations

TLC, thin-layer chromatography; PAHs, polycyclic aromatic hydrocarbons; AnPhNMe$_2$, 4,4',4'',4'''-(anthracene-2,6,9,10-tetrayltetrakis(ethyne-2,1-diyl))tetrakis(N,N-dimethylaniline); AgNP, silver nanoparticle; FETEM, field emission transmission electron microscopy; FESEM, field emission scanning electron microscope; LOD, limit of detection

References

1. (a) Luo, Y.; Zhang, C.; Zheng, B.; Geng, X.; Debliquy, M., Hydrogen sensors based on noble metal doped metal-oxide semiconductor: A review. *Int. J. Hydrog. Energy* **2017,** *42*, 20386-20397; (b) Zhang, M.; Zhen, Y.; Sun, F.; Xu, C., Hydrothermally synthesized SnO2-graphene composites for H2 sensing at low operating temperature. *Mater Sci. Eng. B* **2016,** *209*, 37-44; (c) Chauhan, P. S.; Bhattacharya, S., Hydrogen gas sensing methods, materials, and approach to achieve parts per billion level detection: A review. *Int. J. Hydrog. Energy* **2019,** *44*, 26076-26099.
2. Östergren, I.; Pourrahimi, A. M.; Darmadi, I.; da Silva, R.; Stolaś, A.; Lerch, S.; Berke, B.; Guizar-Sicairos, M.; Liebi, M.; Foli, G., Highly Permeable Fluorinated Polymer Nanocomposites for Plasmonic Hydrogen Sensing. *ACS Appl. Mater. Interfaces* **2021,** *13*, 21724-21732.
3. (a) Singh, S.; Jain, S.; Venkateswaran, P.; Tiwari, A. K.; Nouni, M. R.; Pandey, J. K.; Goel, S., Hydrogen: A sustainable fuel for future of the transport sector. *Renew. Sustain. Energ. Rev.* **2015,** *51*, 623-633; (b) Arnason, B.; Sigfusson, T. I., Iceland—a future hydrogen economy. *Int. J Hydrog. Energy* **2000,** *25*, 389-394; (c) Korotcenkov, G.; Han, S. D.; Stetter, J. R., Review of electrochemical hydrogen sensors. *Chem. Rev.* **2009,** *109*, 1402-1433; (d) Sasaki, K., Why Hydrogen? Why Fuel Cells? In *Hydrogen Energy Engineering*, Springer: 2016; pp 3-14; (e) De Vrieze, J.; Verbeeck, K.; Pikaar, I.; Boere, J.; Van Wijk, A.; Rabaey, K.; Verstraete, W., The hydrogen gas bio-based economy and the production of renewable building block chemicals, food and energy. *New Biotechnol.* **2020,** *55*, 12-18.
4. (a) Lubitz, W.; Tumas, W., Hydrogen: an overview. *Chem. Rev.* **2007,** *107*, 3900-3903; (b) Urs, K. M.; Sahoo, K.; Bhat, N.; Kamble, V., Complementary Metal Oxide Semiconductor-Compatible Top-Down Fabrication of a Ni/NiO Nanobeam Room Temperature Hydrogen Sensor Device. *ACS Appl. Electron. Mater.* **2022,** *4*, 87-91.
5. (a) Abbasi, T.; Abbasi, S., 'Renewable'hydrogen: prospects and challenges. *Renew. Sustain. Energ. Rev.* **2011,** *15*, 3034-3040; (b) Mai, H. D.; Jeong, S.; Nguyen, T. K.; Youn, J.-S.; Ahn, S.; Park, C.-M.; Jeon, K.-J., Pd nanocluster/monolayer MoS2 heterojunctions for light-induced room-temperature hydrogen sensing. *ACS Appl. Mater. Interfaces* **2021,** *13*, 14644-14652.
6. Momirlan, M.; Veziroglu, T., Current status of hydrogen energy. *Renew, Sustain. Energ. Rev.* **2002,** *6*, 141-179.
7. (a) Hübert, T.; Boon-Brett, L.; Black, G.; Banach, U., Hydrogen sensors–a review. *Sens. Actuators Chem.* **2011,** *157*, 329-352; (b) Nag, P.; Majumdar, S.; Bumajdad, A.; Devi, P. S., Enhanced gas sensing performance of tin dioxide-based nanoparticles for a wide range of concentrations of hydrogen gas. *RSC Adv.* **2014,** *4*, 18512-18521.
8. Dutta, S., A review on production, storage of hydrogen and its utilization as an energy resource. *J. Ind. Eng. Chem.* **2014,** *20*, 1148-1156.
9. Lupan, C.; Khaledialidusti, R.; Mishra, A. K.; Postica, V.; Terasa, M.-I.; Magariu, N.; Pauporté, T.; Viana, B.; Drewes, J.; Vahl, A., Pd-functionalized ZnO: Eu columnar films for room-temperature hydrogen gas sensing: a combined experimental and computational approach. *ACS Appl. Mater. Interfaces* **2020,** *12*, 24951-24964.
10. Liu, X.; Cheng, S.; Liu, H.; Hu, S.; Zhang, D.; Ning, H., A survey on gas sensing technology. *Sens.* **2012,** *12*, 9635-9665.
11. (a) Daniel, T. T.; Raveesh, S.; Saikia, K.; Paily, R. P., Magneto-semiconductor resistor for hydrogen detection. *IEEE Sens. J.* **2021,** *21*, 9038-9045; (b) Daniel, T. T.; Yadav, V. K. S.; Abraham, E. E.; Paily, R. P., Carbon Monoxide Sensor Based on Printed ZnO. *IEEE Sens. J.* **2022**, 22, 10910-10917

12. (a) Mahajan, S.; Jagtap, S., Metal-oxide semiconductors for carbon monoxide (CO) gas sensing: A review. *Appl. Mater. Today* **2020,** *18*, 100483; (b) Daniel, T. T.; Majumder, S.; Yadav, V. K. S.; Paily, R., Magnetite-based resistor for nitric oxide detection. *IEEE Sens. J.* **2020,** *20*, 13341-13348.
13. (a) Chang, S.-J.; Hsueh, T.-J.; Chen, I.-C.; Hsieh, S.-F.; Chang, S.-P.; Hsu, C.-L.; Lin, Y.-R.; Huang, B.-R., Highly sensitive ZnO nanowire acetone vapor sensor with Au adsorption. *IEEE Trans. Nanotechnol.* **2008,** *7*, 754-759; (b) Varghese, S. S.; Lonkar, S.; Singh, K.; Swaminathan, S.; Abdala, A., Recent advances in graphene based gas sensors. *Sens. Actuators B Chem.* **2015,** *218*, 160-183; (c) Nikolic, M. V.; Milovanovic, V.; Vasiljevic, Z. Z.; Stamenkovic, Z., Semiconductor gas sensors: Materials, technology, design, and application. *Sens.* **2020,** *20*, 6694.
14. (a) Phanichphant, S., Semiconductor metal oxides as hydrogen gas sensors. *Procedia Eng.* **2014,** *87*, 795-802; (b) Zhang, Z.; Zou, X.; Xu, L.; Liao, L.; Liu, W.; Ho, J.; Xiao, X.; Jiang, C.; Li, J., Hydrogen gas sensor based on metal oxide nanoparticles decorated graphene transistor. *Nanoscale* **2015,** *7*, 10078-10084.
15. (a) Singla, M.; Jaggi, N., Theoretical investigations of hydrogen gas sensing and storage capacity of graphene-based materials: A review. *Sens. Actuators A Phys.* **2021,** *332*, 113118; (b) Kaniyoor, A.; Jafri, R. I.; Arockiadoss, T.; Ramaprabhu, S., Nanostructured Pt decorated graphene and multi walled carbon nanotube based room temperature hydrogen gas sensor. *Nanoscale* **2009,** *1*, 382-386; (c) Ilnicka, A.; Lukaszewicz, J. P., Graphene-based hydrogen gas sensors: A review. *Processes* **2020,** *8* (5), 633.
16. (a) Zhu, Z.; Liu, C.; Jiang, F.; Liu, J.; Liu, G.; Ma, X.; Liu, P.; Huang, R.; Xu, J.; Wang, L., Flexible fiber-shaped hydrogen gas sensor via coupling palladium with conductive polymer gel fiber. *J. Hazard. Mater.* **2021,** *411*, 125008; (b) Zou, Y.; Wang, Q.; Xiang, C.; Tang, C.; Chu, H.; Qiu, S.; Yan, E.; Xu, F.; Sun, L., Doping composite of polyaniline and reduced graphene oxide with palladium nanoparticles for room-temperature hydrogen-gas sensing. *Int. J. Hydrog. Energy* **2016,** *41*, 5396-5404; (c) Wang, P.-C.; Dan, Y.; Liu, L.-H., Effect of thermal treatment on conductometric response of hydrogen gas sensors integrated with HCl-doped polyaniline nanofibers. *Mater. Chem. Phys.* **2014,** *144*, 155-161; (d) Nasirian, S.; Moghaddam, H. M., Hydrogen gas sensing based on polyaniline/anatase titania nanocomposite. *Int. J. Hydrog. Energy* **2014,** *39*, 630-642; (e) Al-Mashat, L.; Debiemme-Chouvy, C.; Borensztajn, S.; Wlodarski, W., Electropolymerized polypyrrole nanowires for hydrogen gas sensing. *J. Phys. Chem. C* **2012,** *116*, 13388-13394; (f) Al-Hartomy, O. A.; Khasim, S.; Roy, A.; Pasha, A., Highly conductive polyaniline/graphene nano-platelet composite sensor towards detection of toluene and benzene gases. *Appl. Phys. A* **2019,** *125*, 1-9; (g) Shah, S. S. A.; Nasir, H.; Saboor, A., Improved dielectric properties of polyetherimide and polyaniline-coated few-layer graphene based nanocomposites. *J. Mater. Sci. Mater. Electron.* **2018,** *29*, 402-411.
17. (a) Ren, Q.; Cao, Y.-Q.; Arulraj, D.; Liu, C.; Wu, D.; Li, W.-M.; Li, A.-D., Resistive-type hydrogen sensors based on zinc oxide nanostructures. *J. Electrochem. Soc.* **2020,** *167*, 067528; (b) Zhao, J.; Wang, W.; Liu, Y.; Ma, J.; Li, X.; Du, Y.; Lu, G., Ordered mesoporous Pd/SnO2 synthesized by a nanocasting route for high hydrogen sensing performance. *Sens. Actuators B Chem.* **2011,** *160*, 604-608; (c) Boudiba, A.; Roussel, P.; Zhang, C.; Olivier, M.-G.; Snyders, R.; Debliquy, M., Sensing mechanism of hydrogen sensors based on palladium-loaded tungsten oxide (Pd–WO3). *Sens. Actuators B Chem.* **2013,** *187*, 84-93; (d) Sanger, A.; Kumar, A.; Kumar, A.; Jaiswal, J.; Chandra, R., A fast response/recovery of hydrophobic Pd/V2O5 thin films for hydrogen gas sensing. *Sens. Actuators B Chem.* **2016,** *236*, 16-26.
18. (a) Zhou, W.; Li, W.; Wang, J.-Q.; Qu, Y.; Yang, Y.; Xie, Y.; Zhang, K.; Wang, L.; Fu, H.; Zhao, D., Ordered mesoporous black TiO2 as highly efficient hydrogen evolution photocatalyst. *J. Am. Chem. Soc.* **2014,** *136*, 9280-9283; (b) Boudiba, A.; Zhang, C.; Umek, P.; Bittencourt, C.; Snyders, R.; Olivier, M.-G.; Debliquy, M., Sensitive and rapid hydrogen sensors based on Pd–WO3 thick films with different morphologies. *Int. J. Hydrog. Energy* **2013,** *38*, 2565-2577.
19. Daniel, T. T.; Saikia, K.; Raveesh, S.; Paily, R., Hydrogen Sensing of Heterostructured Magnetic Nanospheres With Different Fe to Zn Molar Ratio. *IEEE Trans. Nanotechnol.* **2021,** *20*, 669-677.
20. Punetha, D.; Kar, M.; Pandey, S. K., A new type low-cost, flexible and wearable tertiary nanocomposite sensor for room temperature hydrogen gas sensing. *Sci. Rep.* **2020,** *10*, 1-11.
21. (a) Islam, K.; Narjinari, H.; Kumar, A., Polycyclic Aromatic Hydrocarbons Bearing Polyethynyl Bridges: Synthesis, Photophysical Properties, and their Applications. *Asian J. Org. Chem.* **2021,** *10*, 1544-1566; (b) Jhulki, S.; Moorthy, J. N., Small molecular hole-transporting materials (HTMs) in organic light-emitting diodes (OLEDs): structural diversity and classification. *J. Mater. Chem. C* **2018,** *6*, 8280-8325; (c) Chen, M.; Yan, L.; Zhao, Y.; Murtaza, I.; Meng, H.; Huang, W., Anthracene-based semiconductors for organic field-effect transistors. *J. Mater. Chem. C* **2018,** *6*, 7416-7444.
22. (a) Islam, K.; Narjinari, H.; Bisarya, A.; Kumar, A., Multi-fold Sonogashira coupling: a new and convenient approach to obtain tetraalkynyl anthracenes with tunable photophysical properties. *Org. Biomol. Chem.* **2021,** *19*, 9692-9704; (b) Islam, K.; Bhunia, B. K.; Mandal, G.; Nag, B.; Jaiswal, C.; Mandal, B. B.; Kumar, A., Room-Temperature, Copper-Free, and Amine-Free Sonogashira Reaction in a Green Solvent: Synthesis of

Tetraalkynylated Anthracenes and *In Vitro* Assessment of Their Cytotoxic Potentials. *ACS Omega* **2023**, DOI: doi.org/10.1021/acsomega.3c00732; (c) Islam, K.; Arora, V.; Vikas, V.; Nag, B.; Kumar, A. Nickel Bromide Catalyzed Ligand-Free and Activator-less Suzuki Coupling Reactions. *ChemCatChem* 2022, *14*, No. e202200440
23. Daniel, T. T.; Yadav, V. K. S.; Natu, G.; Paily, R., Fully printed inorganic schottky diode. *IEEE Electron Device Lett.* **2021,** *42* (8), 1212-1215.
24. Palathinkal, J. R.; Majumder, S.; Daniel, T. T.; Yadav, V. K. S.; Palathinkal, R. P. In Fabrication of Se-Fe 2 O 3-based Schottky Diode Using Cantilever-based Ag-contact Printing Technology: Topic: NS/NC-Non-silicon and Non-CMOS, 2022 33rd Annual SEMI Advanced Semiconductor Manufacturing Conference (ASMC), IEEE: 2022; pp 1-5.